Science Advances
AAAS

advances.sciencemag.org/cgi/content/full/6/51/eabd5109/DC1

Supplementary Materials for

Reduced tropical cyclone densities and ocean effects due to anthropogenic greenhouse warming

Jung-Eun Chu, Sun-Seon Lee*, Axel Timmermann*, Christian Wengel, Malte F. Stuecker, Ryohei Yamaguchi

*Corresponding author. Email: sunseonlee@pusan.ac.kr (S.-S.L.); axel@ibsclimate.org (A.T.)

Published 16 December 2020, *Sci. Adv.* **6**, eabd5109 (2020)
DOI: 10.1126/sciadv.abd5109

This PDF file includes:

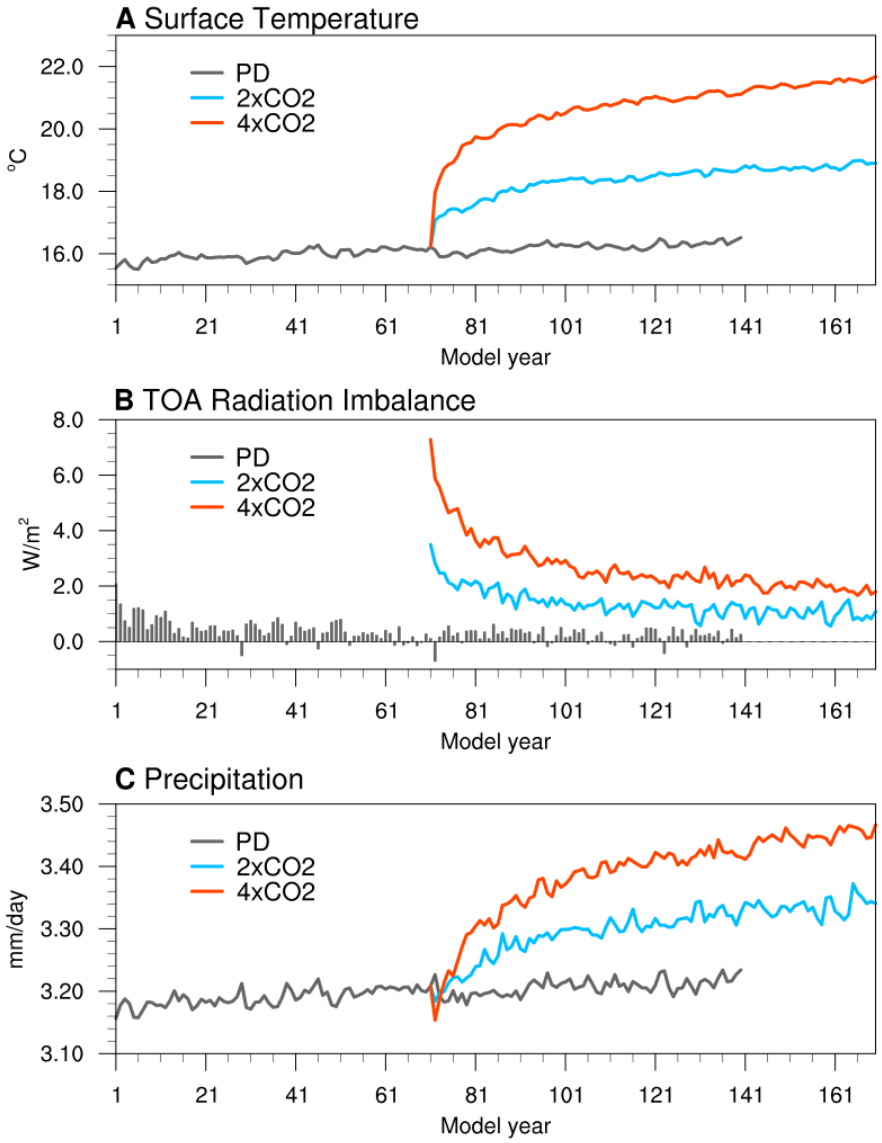

Fig. S1. Time series of the century-long global climate response to CO_2 concentration. Time series of the global and annual mean climate response. (A) Surface air temperature (°C), (B) net radiation imbalance at top of the atmosphere (TOA) (positive downward, W m^{-2}), and (C) precipitation (mm day^{-1}). Gray colors denote quantities for 140 years of the PD condition, and blue and red lines indicate 100 years of doubling CO_2 ($2\times CO_2$) and quadrupling CO_2 ($4\times CO_2$) experiments started from year 71 of PD, respectively.

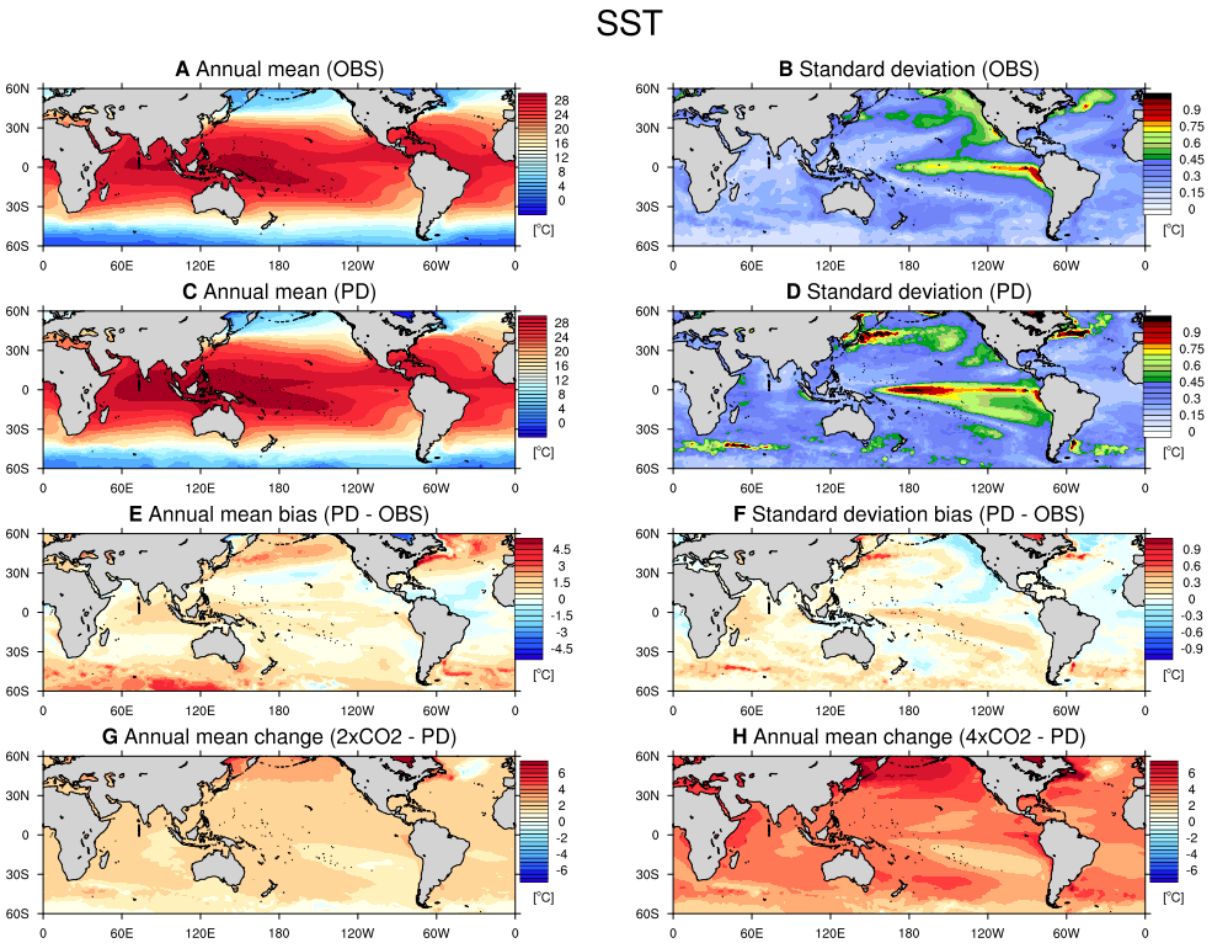

Fig. S2. Spatial distribution of the sea surface temperature (SST) from observations and model simulations. (A and C) Annual mean SST (°C) climatology from (A) observation and (C) PD condition. (B and D) Standard deviation of the annual mean SST from (B) observation and (D) PD condition. (E and F) Model bias in (E) annual mean SST and (F) standard deviation. (G and H) Changes in annual mean SST in (G) $2\times CO_2$ and (H) $4\times CO_2$ relative to PD. Observational data is from HadISST for the 1990-2018 period. Last 20 years of the simulation data are used. Long-term linear trends were removed before any statistical analysis.

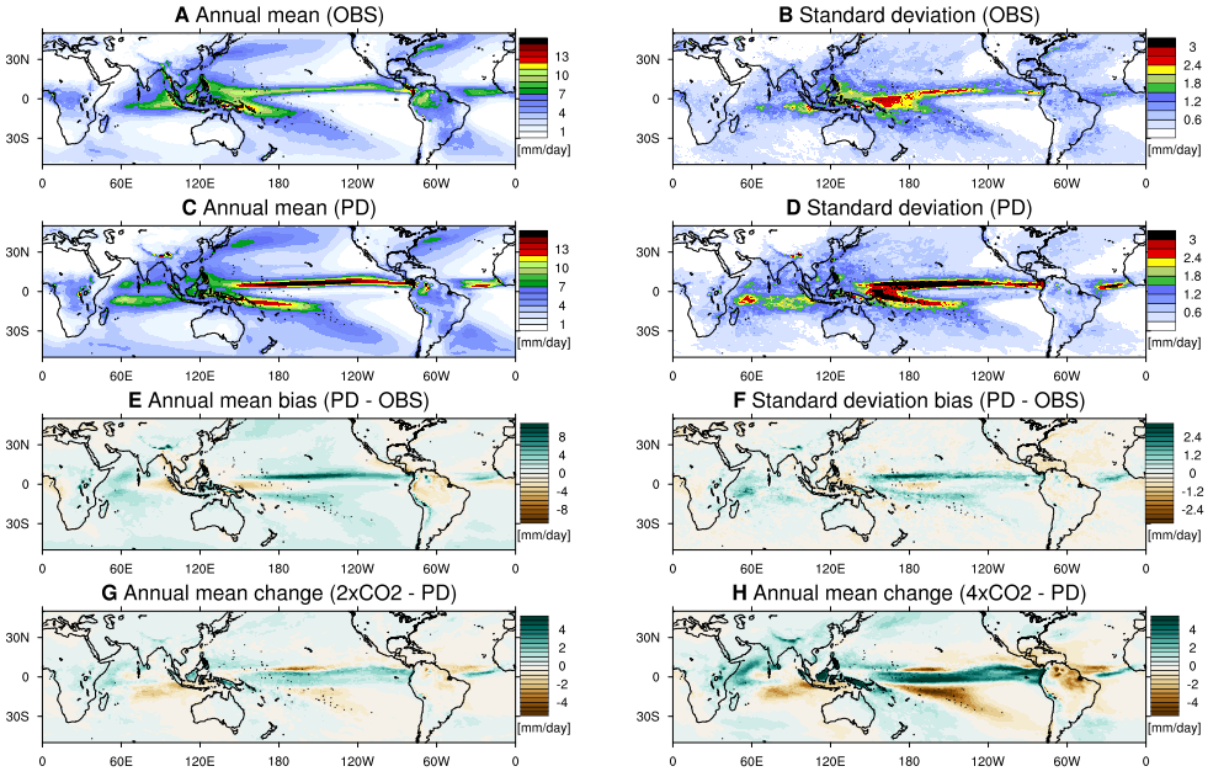

Fig. S3. Spatial distribution of the precipitation from observation and model simulations. (A and C) Annual mean precipitation (mm day^{-1}) climatology from (A) observation and (C) PD condition. (B and D) Standard deviation of the annual mean precipitation from (B) observation and (D) PD condition. (E and F) Model bias in (E) annual mean precipitation and (F) standard deviation. (G and H) Changes in annual mean precipitation in (G) $2\times CO_2$ and (H) $4\times CO_2$ relative to PD. Observational data is from the Tropical Rainfall Measurement Mission (TRMM) 3B43 product during the 1999-2018 period.

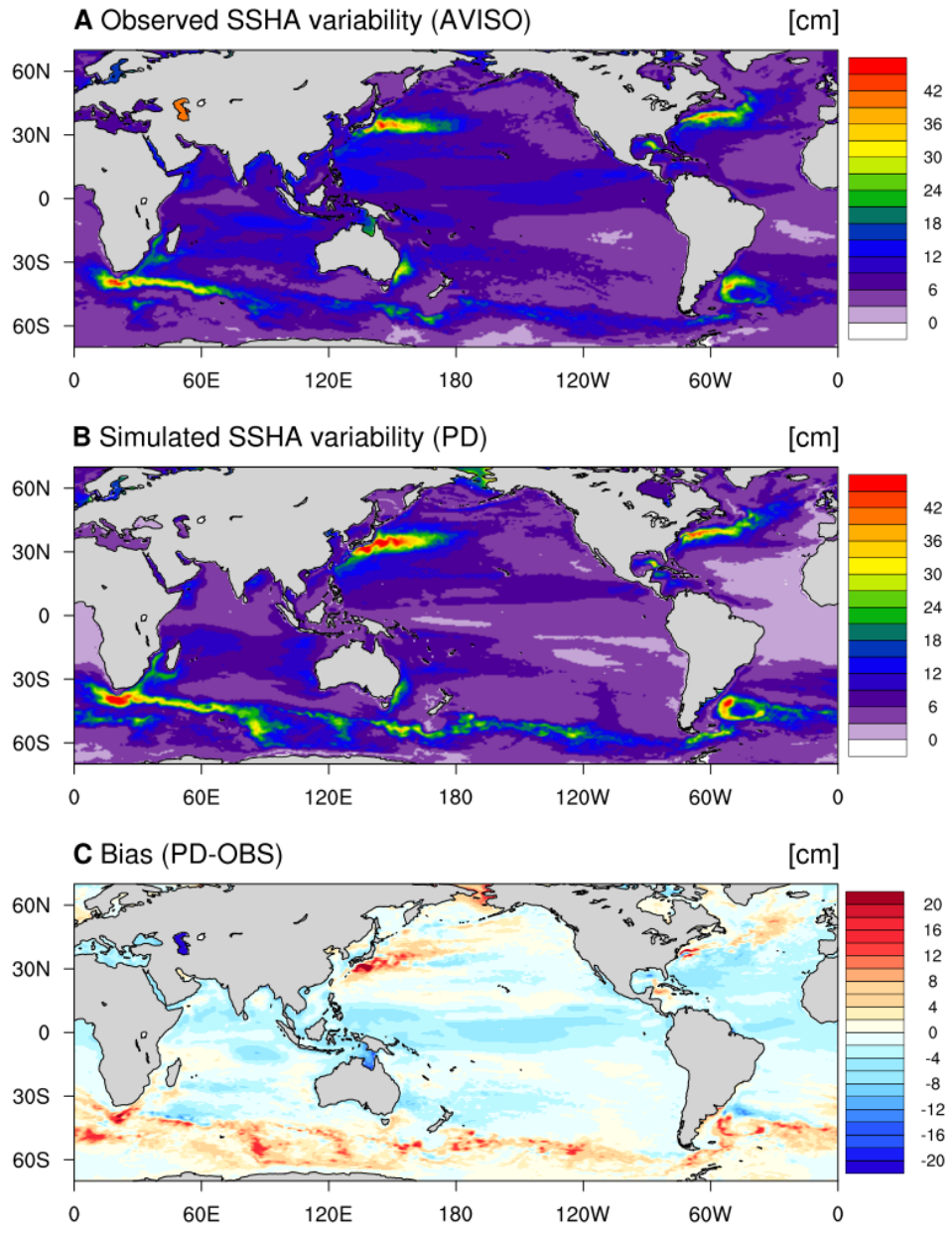

Fig. S4. Daily sea surface height variability from observation and model simulation. Standard deviation of the daily sea surface height anomaly (SSHA) from (A) observation, (B) PD simulation and (C) difference between PD and observation. Observational data is obtained from Archiving, Validation and Interpretation of Satellite Oceanographic Data (AVISO) merged product during the 1993-2018 period.

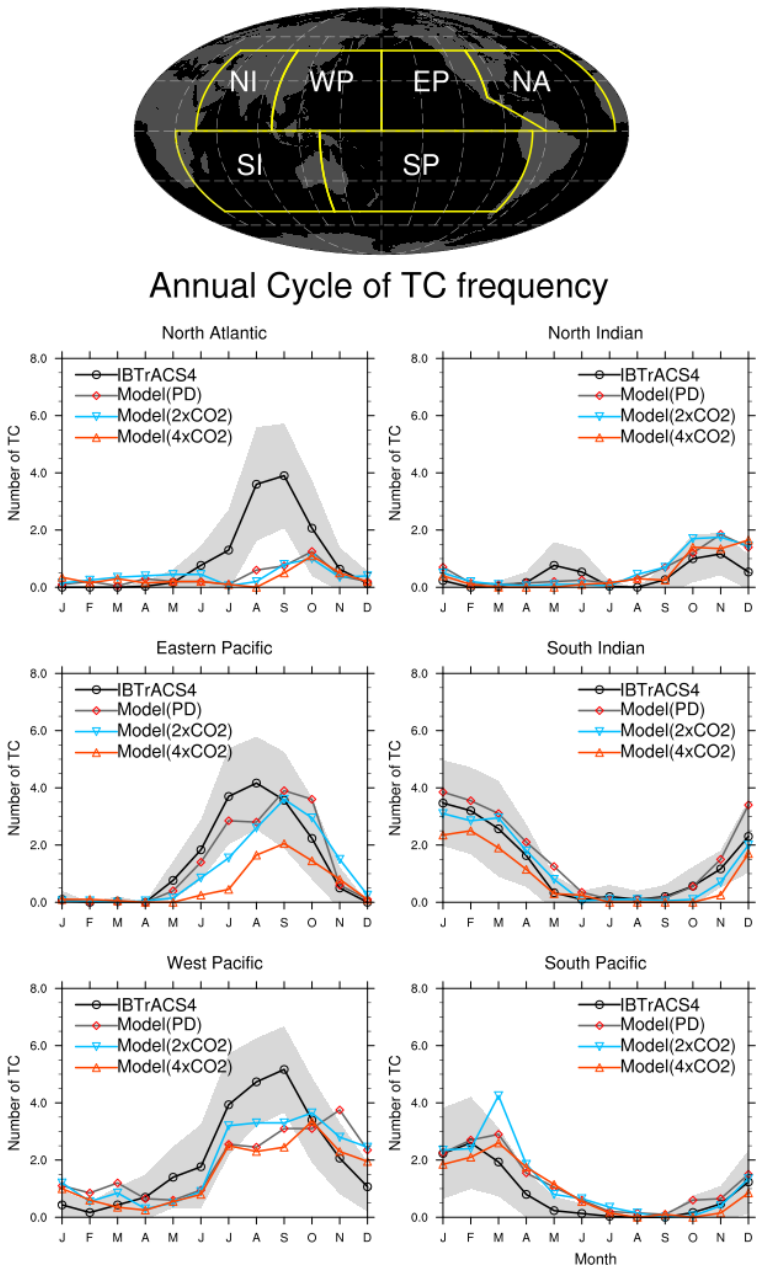

Fig. S5. Annual cycle of the monthly TC frequency per basin. The domain of each basin (upper) and the annual cycle of monthly TC frequency (year^{-1}) from observations (black), PD (gray), 2×CO_2 (blue), and 4×CO_2 (red) simulations. Gray shadings show the range of year-to-year variability of TC frequency at each month in the observation.

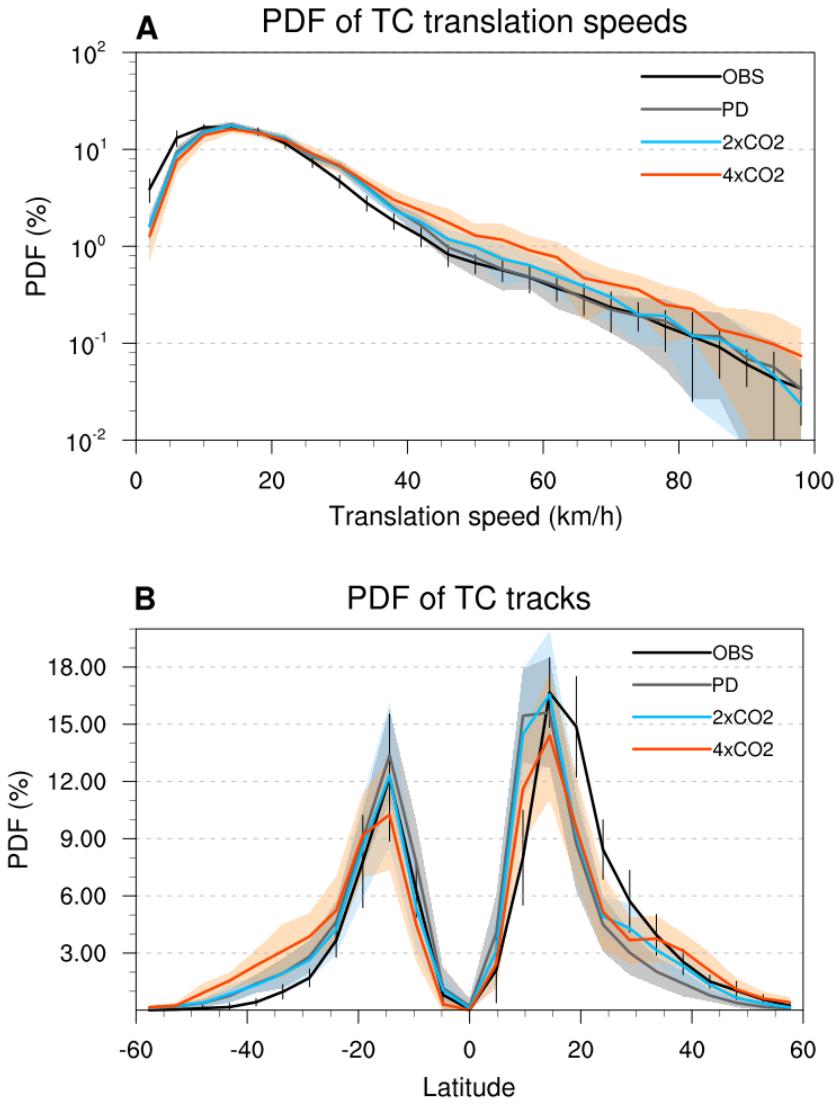

Fig. S6. Probability density distributions (PDFs) of TC translation speeds and track latitude.

(A) TC translation speeds and (B) track latitude in observations (black), PD (gray), 2×CO_2 (blue), and 4×CO_2 (red) experiments. Vertical bars indicate one standard deviation of interannual variability in the observation and shadings indicate one standard deviation of interannual variability for the simulations.

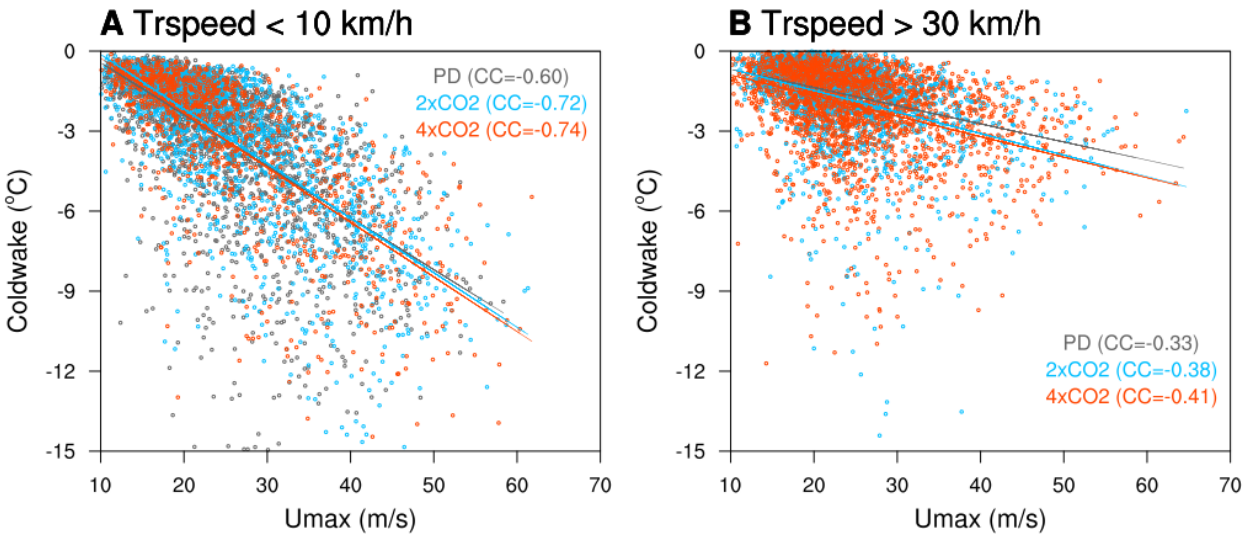

Fig. S7. Relationship between cold wakes and maximum wind speed. The magnitude of cold wakes as a function of wind speed for (A) slow-moving TCs with translation speed of less than 10 km h^{-1} and (B) fast-moving TCs with translation speed of greater than 30 km h^{-1} in the PD (gray), 2×CO_2 (blue), and 4×CO_2 (red) experiments.

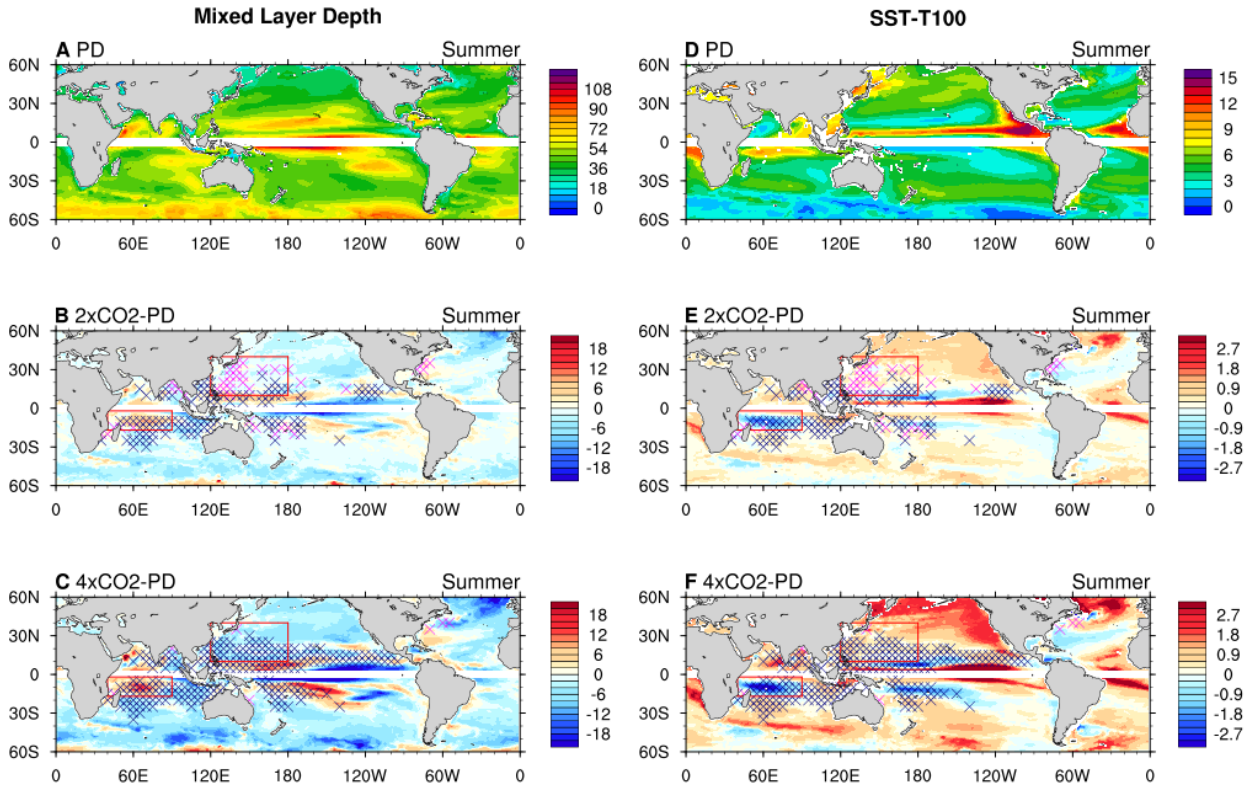

Fig. S8. Changes in mixed layer depth and upper ocean vertical temperature gradient. Global distribution of the summertime (A-C) mixed layer depth and (D-F) ocean vertical temperature difference between surface and 100-m depth. (A,D) Climatological condition from PD experiment, and changes in (B,E) 2×CO_2 and (C,F) 4×CO_2 experiments compared to PD. Summer mean is computed over June-November for the Northern Hemisphere and December-May for the Southern Hemisphere. Cross-hatched areas in (B,C,E,F) indicate changes in TC density greater than 10 hours day^{-1}. Magenta color indicates an increase TC density whereas navy color indicates a decrease. Red box in (B,C,E,F) indicates area of tropical Indian Ocean and western North Pacific used in Fig. S9.

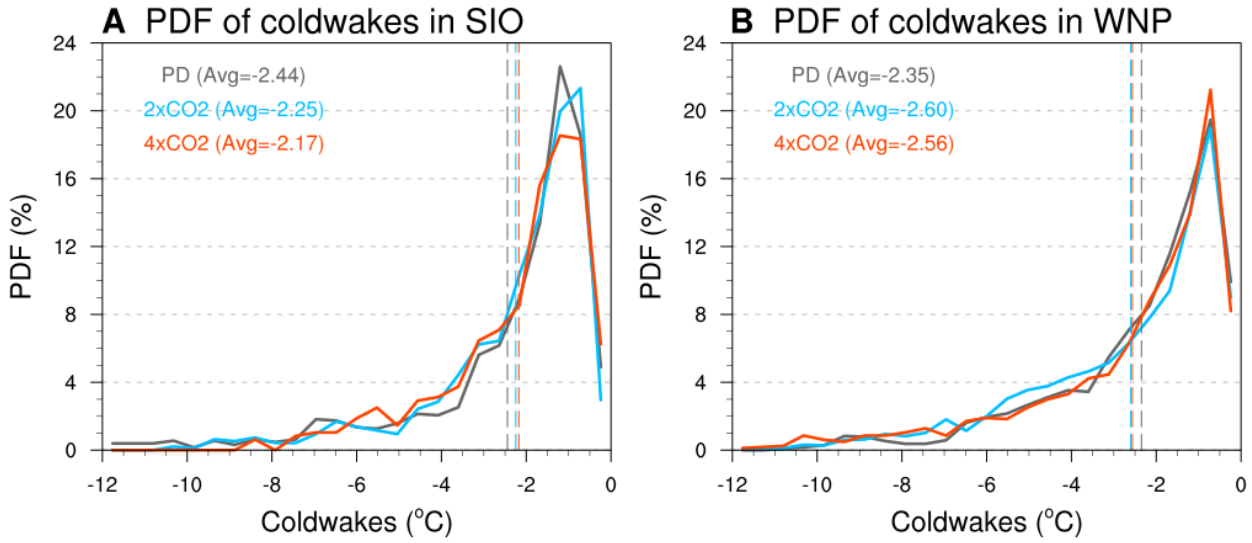

Fig. S9. PDFs of TC-induced cold wakes. PDFs of the cold wakes from the PD (gray), 2×CO_2 (blue), and 4×CO_2 (red) experiments over the (A) southern Indian Ocean (17 °S–2 °S, 40°E–90°E) and (B) in western North Pacific (10 °N–40°N, 120°E–180°E). Dashed vertical lines indicate mean cold wakes in each experiment.

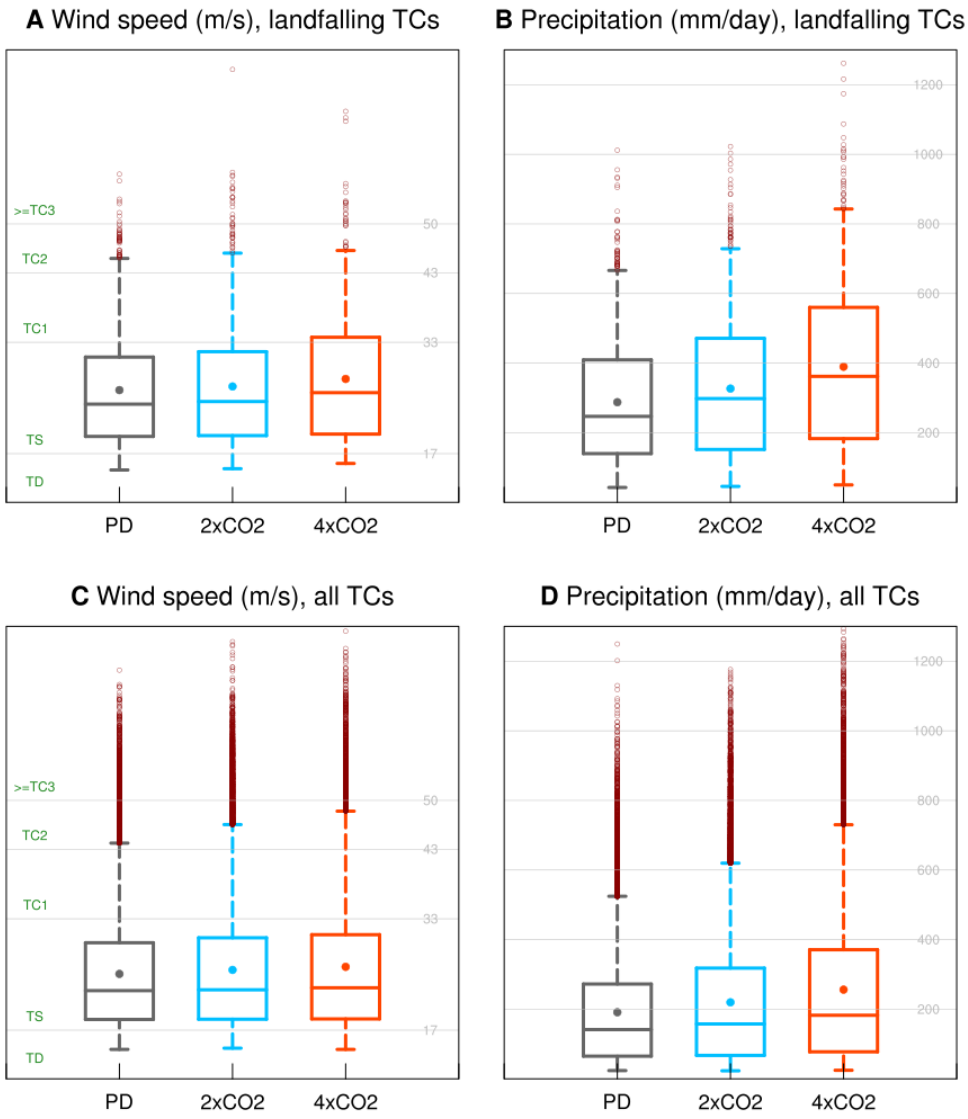

Fig. S10. Box diagrams of TC intensity and precipitation for the present-day and warmer climate simulations. Box plots of (A and C) maximum wind speed (m s^{-1}) and (B and D) precipitation (mm day^{-1}) for (A and B) landfalling TCs and (C and D) all TCs in the PD (gray), 2×CO_2 (blue), and 4×CO_2 (red) experiments. The limits of whiskers represent the 5th and 95th percentiles. The limits of boxes represent the 25th and 75th percentiles. The line and circle inside the boxes indicate median and mean, respectively. Values above 95th percentiles line are marked as the open circles. To remove the impact of extratropical storms, TCs within 30 °S to 30 °N are considered.

Table S1. Summary of observed and simulated TC statistics. TC-related statistics for (A) observations, as well as the (B) PD, (C) 2×CO_2, and (D) 4×CO_2 experiments. Shown are the annual number of TCs, mean duration (days), mean travel distance (km), mean translation speed (km h^{-1}), and mean maximum wind speed (m s^{-1}). Values on the right of plus-minus sign (±) indicate the year-to-year standard deviation.

	(A) OBS (IBTrACS4)	(B) PD	(C) 2×CO_2	(D) 4×CO_2
nTC per year (≥TS)	85±9	85±11	79±9	58±6
mean duration (days)	9.0±0.9	6.9±0.5	6.5±0.5	5.9±0.5
mean travel distance (km)	3882±429	3196±252	3087±313	3005±328
mean translation speed (km h^{-1})	18.0±0.7	19.3±0.8	19.7±0.9	21.4±1.3
mean maximum wind speed (m s^{-1})	39.3±1.7	32.9±1.0	33.6±1.2	34.7±1.6

Table S2. List of observed cold wakes. The name of the TC, maximum SST cooling, latitude of the maximum cooling, and references.

Number	TC Name (year)	Maximum cooling (°C)	Latitude	Reference
1	Soulik (2018)	8.1	32 °N	*(40)*
2	Lupit (2010)	3.8	20 °N	*(39)*
3	Fanapi (2010)	2.5	24 °N	*(39)*
4	Malakas (2010)	3.0	24 °N	*(39)*
5	Megi (2010)	7.0	19 °N	*(39)*
6	Frances (2010)	2.1	22 °N	*(39)*
7	Ma-on (2011)	4.3	24 °N	*(41)*
8	Muifa (2011)	3.5	22 °N	*(41)*
9	Talas (2011)	1.1	24 °N	*(41)*
10	Kulap (2011)	1.0	20 °N	*(41)*
11	Roke (2011)	0.8	22 °N	*(41)*
12	Bolaven (2012)	2.0	20 °N	*(41)*
13	Sanba (2012)	0.8	24 °N	*(41)*
14	Prapiroon (2012)	3.3	22 °N	*(41)*
15	Kai-Tak (2000)	10.8	20 °N	*(16)*